Passively Q-switched Yb:YAG laser with Cr^{4+}:YAG as the saturable absorber

Jun Dong, Peizhen Deng, Yupu Liu, Yinghua Zhang, Jun Xu, Wei Chen, and Xinglong Xie

By using a continuous-wave Ti:sapphire laser as a pumping source, we demonstrated a passively Q-switched Yb:YAG laser at room temperature with Cr^{4+}:YAG as the saturable absorber. We achieved an average output power of as much as 55 mW at 1.03 μm with a pulse width (FWHM) as short as 350 ns. The initial transmission of the Cr^{4+}:YAG has an effect on the pulse duration (FWHM) and the repetition rate of the Yb:YAG passively Q-switched laser. The Yb:YAG crystal can be a most promising passively Q-switched laser crystal for compact, efficient, solid-state lasers.

OCIS codes: 140.3540, 140.5680, 140.3580.

1. Introduction

Passively Q switching of solid-state lasers is usually accomplished with organic dyes or color centers as saturable absorbers. Dyes,[1] however, have poor thermal stability and tend to degrade rapidly. To operate in cw-pumped lasers, dyes require a circulation system. Color centers, such as the color-center LiF crystal,[2] exhibit a fading phenomenon. Recently, chromium-doped host crystals, such as YAG,[3] GSGG,[4] and forsterite,[5] have been used as passive Q switches for Nd^{3+}-doped crystal solid-state lasers. Compared with Nd ions in laser crystals, the Yb ion is ideally suited for diode pumping because it has a simple energy-level scheme with the necessary properties for a laser system. Furthermore, diode-pumped Yb:YAG lasers have several advantages relative to Nd:YAG lasers, such as a long storage lifetime (951 μs),[6] a very low quantum defect (8.6%) that results in three times less heat generation during lasing than comparable Nd-based laser systems,[7] large absorption width around the InGaAs laser emission range,[8] a relatively large emission cross section, easy growth of high quality and moderate concentration crystal without concentration quenching, and strong energy-storing capacity. Another advantage of using Yb:YAG is that the 940-nm absorption feature is approximately five times broader than the 808-nm absorption feature in Nd:YAG, and, therefore, the Yb:YAG system is less sensitive to diode wavelength specifications.[9] Several researchers have reported on Q-switched Yb:YAG lasers by use of the electro-optic Q switch[10] and a semiconductor saturable absorber mirror (SESAM).[11] Fan *et al*.[10] reported an output energy of as much as 72 μJ/pulse at 1.03 μm with a pulse length as short as 11 ns FWHM. To our knowledge Spühler *et al*. reported the first Yb:YAG microchip laser that was passively Q switched with a SESAM. Pulses of 1.1-μJ energy with a pulse width of 530 ps and a peak power of 2.1 kW at a repetition rate of 12 kHz were obtained.

We present a passively Q-switched operation using Cr^{4+}:YAG as the saturable absorber in a Ti:sapphire laser-pumped Yb:YAG laser. In comparison with a SESAM, doped bulk crystals as saturable absorbers have several advantages such as high damage threshold, low cost, and simplicity. Absorbers with such advantages can lead to the development of more efficient, compact Q-switched solid-state lasers.

2. Experiments

The experimental setup of the Ti:sapphire laser-pumped Yb:YAG passively Q-switched laser with Cr^{4+}:YAG as the saturable absorber is shown in Fig. 1. The Mira 900 tunable Ti:sapphire laser with an output power of as much as 1 W was used as the pump source. The optical pump system was composed of a spherical lens ($f = 75$ mm) for focusing the pump beam to an approximately 50-μm-diameter circular spot. After the addition of the focusing sys-

The authors are with the Shanghai Institute of Optics and Fine Mechanics, Chinese Academy of Sciences, P.O. Box 800-211, Shanghai 201800, China.

Received 13 April 2000; revised manuscript received 8 January 2001.

0003-6935/01/244303-05$15.00/0

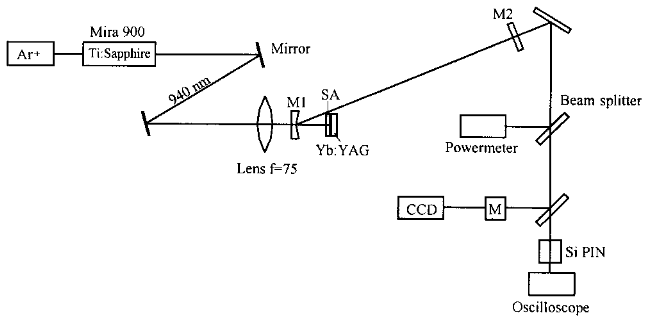

Fig. 1. Schematic of a Ti:sapphire laser-pumped Yb:YAG passively Q-switched laser: M1, M2, cavity mirrors; M, monochromator, CCD, charge-coupled device array; SA, saturable absorber.

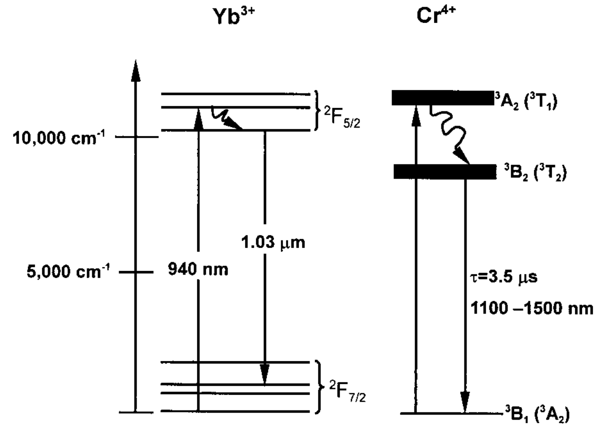

Fig. 2. Energy levels of Yb^{3+} and Cr^{4+} and relaxation mechanisms. τ represents the lifetime of the $^3B_2$ level.

tem, the pump power was measured to be as much as 920 mW. The laser cavity was configured to be semispherical and was formed by the 50-mm radius of curvature mirror M1 and flat mirror M2. Mirror M1, with one face coated for high transmission at 940 nm and the other face coated for high transmission at 940 nm and total reflection at 1.03 μm, was placed on the front of the input facet of the Yb:YAG crystal. The Yb:YAG gain medium was doped with 20-at. % Yb^{3+}; the material properties of Yb:YAG are summarized in Table 1. The 0.5-mm-thick Yb:YAG gain element is polished flat and parallel, is coated on one face of the crystal for high transmission at 940 nm and at 1030 nm, and the other surface of the crystal is coated for total reflection at 940 nm and at 1030 nm. Mirror M2, coated for total reflection at 940 nm and reflectivity of 97% at 1.03 μm, acted as an output coupler. The overall cavity length is 23 cm. More than 90% of the laser pump power was absorbed by the Yb:YAG crystal. We performed the laser operation at 278 K by using the constant-temperature water-cooled circulation with a copper surface. We recorded the Q-switched pulses by using a fast Si P-I-N detector with a 1.5-ns rise time and a Tektronix TDS 380 digitizing oscilloscope with a 400-MHz sampling rate in the single-shot mode. The output power was measured with a laser powermeter.

Table 1. Material Properties of Yb^{3+}:YAG Crystal

Parameters	Yb^{3+}:YAG
Doping concentration	26.6×10^{20} cm^{-3}
Pump wavelength	940 nm
Laser wavelength	1030 nm
Absorption bandwidth	19 nm
Emission bandwidth	9 nm
Upper-state lifetime	951 nm
Emission cross section	2.0×10^{-20} cm^2
Absorption cross section	0.8×10^{-20} cm^2
Saturation intensity	28 kW/cm^2
Thermal conductivity	0.13 W/cmK
dn/dt	8.9×10^{-6} K^{-1}
Refractive index	1.823

3. Results and Discussion

Figure 2 shows the energy-level schemes of Cr^{4+} and Yb^{3+} and the involved relaxation mechanisms. Without the Cr^{4+}:YAG crystal in the laser cavity, a maximum cw output power of 138 mW was obtained at 1.03 μm with a slope efficiency of 35% with respect to an absorbed pump power of 738 mW. The passively Q-switched Yb:YAG operation was achieved with the insertion of Cr^{4+}:YAG crystals into the laser cavity. In our experiments, three 0.5-mm-thick Cr^{4+}:YAG crystals with small-signal transmission of 85%, 90%, and 95% were used as saturable absorbers. The Cr^{4+}:YAG saturable absorber was attached tightly to the Yb:YAG sample. The average output power, repetition rate, and pulse width in a Q-switched mode were measured as functions of absorbed pump power. The pulse energy was determined from the average output power and repetition rate. The peak power was determined from the pulse energy and pulse width. Figure 3 shows the average output power, pulse energy, and peak power as functions of the absorbed pump power for saturable absorbers with three small-signal transmissions. From Fig. 3 we can see that the average output power depends linearly on the absorbed pump power for three initial transmissions of Cr^{4+}:YAG crystals with the exception of the 95% transmission when the pump power is greater than 600 mW. From the linear relationship of absorbed pump power and average output power, the pump threshold can be extrapolated. The pumping threshold powers are approximately 350, 410, and 390 mW with a decrease in the initial transmission of Cr^{4+}:YAG from 95% to 85%. The actual pumping threshold for the saturable absorber with $T_0 = 85\%$ should be higher than that for $T_0 = 90\%$ because the insertion loss of $T_0 = 85\%$ is greater than that of $T_0 = 90\%$. This phenomenon could be the error that exists in the experiment for which the actual cause is unknown. The slope efficiencies for three T_0 are nearly the same at approximately 15%, and the highest optical efficiency (the ratio of output power and pump power) of the pas-

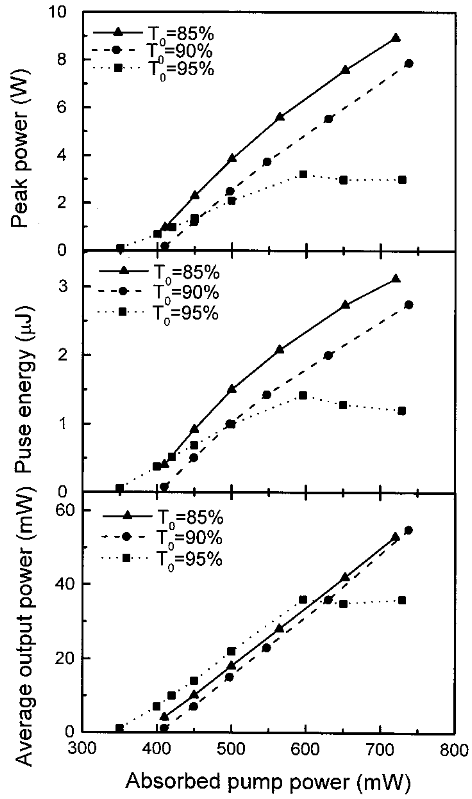

Fig. 3. Average output power, pulse energy, and peak power versus absorbed pump power for three Cr^{4+}:YAG saturable absorbers with different small-signal transmissions.

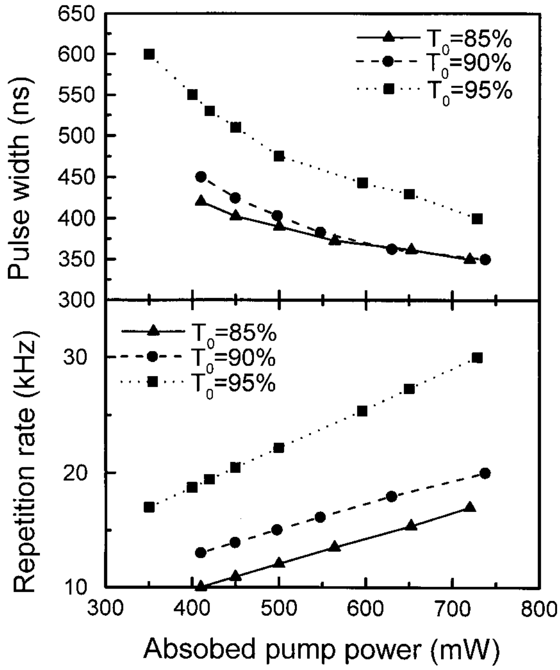

Fig. 4. Repetition rate and pulse width versus absorbed pump power for different Cr^{4+}:YAG saturable absorbers with different small-signal transmissions.

sively Q-switched lasers is approximately 7%. The highest average output power is obtained with a $T_0 = 90\%$ Cr^{4+}:YAG crystal at a maximum pump power of 738 mW and the Yb:YAG laser generates an average output power of 55 mW. And the average output power is unchanged for 95% initial transmission of Cr^{4+}:YAG with an increase in the pump power when the input power is greater than 600 mW, which could be the result of higher initial transmission of the saturable absorber although the actual reasons are not clear. We obtained 3.2-μJ Q-switched pulses with a pulse width of 350 ns, resulting in a peak power of approximately 9 W at a repetition rate of 17 kHz with $T_0 = 85\%$ at 720-mW absorbed pump power (Fig. 3).

Figure 4 shows the pulse repetition rate and the pulse width as functions of the absorbed pump power for three small-signal transmissions of Cr^{4+}:YAG crystals. For the $T_0 = 95\%$ Cr^{4+}:YAG crystal, we obtained 400-ns pulses with a repetition rate of 30 kHz at a maximum absorbed pump power of 730 mW. The corresponding pulse energy and peak power were approximately 1.3 μJ and 3 W, respectively. As the saturable absorbers with a lower initial transmission were used, we obtained pulses with higher peak power, a shorter pulse width, and lower repetition rates. We generated a pulse width of 350 ns with a repetition rate of 20 kHz by using a $T_0 = 90\%$ Cr^{4+}:YAG laser, which corresponds to a pulse energy of 2.75 μJ and a peak power of 8 W at the maximum absorbed pump power of 738 mW. The highest pulse energy and peak power were generated when we used the saturable absorber with initial transmission of 85%. At a maximum absorbed pump power of 720 mW, we detected pulses of 350-ns duration with a repetition rate of 17 kHz. The highest pulse energy and peak power are 3.2 μJ and 9 W. From Fig. 4 we can see that the pulse width and the pulse repetition rates of each Q-switched pulse correlate with the absorbed pump power and the saturable absorber initial transmission T_0 when the output coupler reflectivity remains the same. With a saturable absorber of high initial transmission, the Q-switched laser has a high repetition rate and a broad pulse width; with a saturable absorber of low initial transmission, the Q-switched laser has a short pulse width and a low repetition rate. Figure 5 shows a typical oscilloscope trace of a train of pulses with a pulse repetition of approximately 14 kHz. From Fig. 5 we can see that the pulses are stable. Figure 6 shows a typical single Q-switched laser pulse with 3.2-μJ energy and a 0.35-μs pulse duration (FWHM) at a pulse repetition rate of 17 kHz for 85% small-signal transmission at the maximum absorbed pump power of 720 mW. The corresponding peak power is approximately 9 W.

When the absorption cross section of the saturable absorber (6.2×10^{-18} cm^2 for Cr^{4+}:YAG) is much greater than the cross section of the lasing transition (2.0×10^{-20} cm^2 for Yb^3:YAG), the resulting pulse width is[12,13]

$$t_p = \frac{0.86 t_{\mathrm{rt}}}{\gamma_{\mathrm{sat,rt}}} \left[\frac{\delta(1+\delta)\eta}{\delta - \ln(1+\delta)} \right],$$

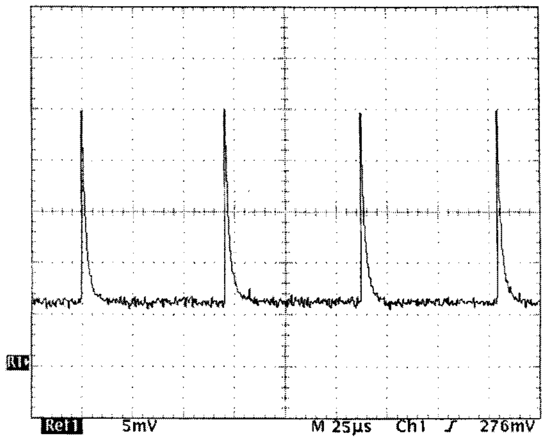

Fig. 5. Oscilloscope trace of a train of passively Q-switched pulses of Yb:YAG crystal with a repetition rate of approximately 14 kHz.

where t_{rt} is the round-trip time of light within the laser cavity, η is the energy extraction efficiency of the laser pulse given by the relationship $\eta(1 + \delta) = -\ln(1 - \eta)$, and $\delta = \gamma_{sat,rt}/(\gamma_{par,rt} + \gamma_{op})$ is the ratio of saturable-to-unsaturable cavity losses, where $\gamma_{sat,rt}$ is the round-trip saturable loss constant, $\gamma_{par,rt}$ is the round-trip unsaturable intracavity parasitic loss constant, and γ_{op} is the output coupling loss constant. For our Cr^{4+}:YAG passively Q-switched Yb:YAG laser experiments, we estimated the parasitic loss $\gamma_{par,rt} = 0.03$ by taking into account the reflectivity of the Cr^{4+}:YAG surface, the upper limit for the saturable loss $\gamma_{sat,rt} = 0.02$. By taking into account the output loss $\gamma_{op} = 0.03$ and $t_{rt} = 1.53$ ns, we calculated that $t_p = 320$ ns, which is in good agreement with the experimental result of 350 ns. Some disparity exists between the measured and the calculated pulse widths because of the inaccurate determination of the unsaturated intracavity parasitic loss constant. From this point of view, higher peak power can be generated by use of a shorter cavity length and a more powerful diode pumping source.

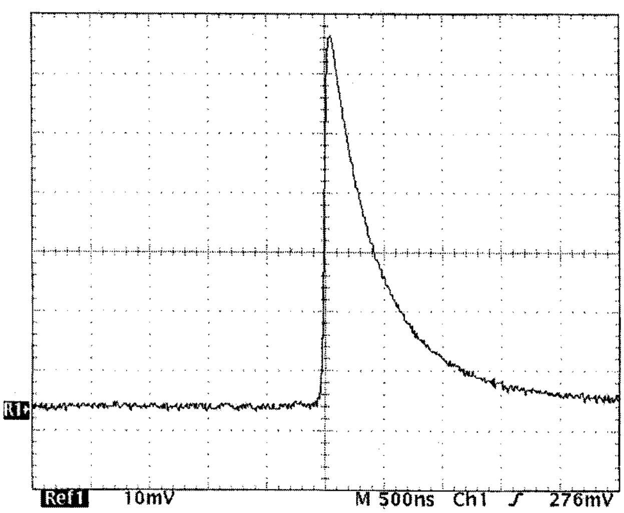

Fig. 6. Oscilloscope trace of a single Q-switched pulse with a 350-ns pulse duration at 17-kHz repetition rate when the pump power is 720 mW for $T_0 = 85\%$ Cr^{4+}:YAG.

The relatively higher pumping threshold comparable to Nd:YAG is due to the reabsorption of Yb^{3+} and absorption of Cr^{4+} at 1.03 μm. A lower slope efficiency comparable with Nd:YAG could be the result of thermal lensing and the oscillation cavity design that we used for the experiment. In theory, thermal lensing in laser materials is usually caused by the quantum defect between the energies of the absorbed pump photon and the output laser photon. Thus laser materials with a minimal difference between the pump wavelength and the laser output wavelength could be expected to have lower heating as long as nonradiative sites, concentration quenching, excited-state absorption, and upconversion are weak. The Yb:YAG lasers are pumped at either 941 or 968 nm and oscillate at 1.03 μm. The quantum defect of Yb:YAG is lower than that of Nd:YAG and heat generation is three times lower than that of Nd:YAG.[7] However, there are other absorption processes that can heat the Yb:YAG without contributing to pumping the $^2F_{5/2}$ level of the Yb ions: (1) UV absorption of color centers, (2) IR absorption of hydroxyl groups, and (3) absorption by impurity atoms such as Ho and Er. The results reported in Ref. 14 show that the color centers, hydroxyl groups, and impurities exist in Yb:YAG crystal although the dislocation density is low. Theoretically, the doping concentration of Yb^{3+} in YAG can be very high; in practice, a high doping level of Yb^{3+} in YAG crystal introduces additional Ho^{3+} and Er^{3+} ions. The increased concentration of Ho^{3+} and Er^{3+} reduced the fluorescence lifetime of Yb^{3+} and lowered laser efficiency to $\eta = \tau_f/\tau_0$.[15] Because energy transfer from the laser upper level $^2F_{5/2}$ of Yb^{3+} to $^4I_{11/2}$ of Er^{3+} and $^5I_6$ of Ho^{3+} can take place directly or assisted by phonons, the energy transfer efficiency is high.[16,17] Sumida and Fan[6] investigated the dependence of the Yb^{3+} lifetime on doping concentration in Yb:YAG crystals and found that the lifetime was shortened when the Yb^{3+} doping concentration increased (>15 at. %) and was reduced to approximately 15% when the doping concentration was 25 at. %. For the Yb:YAG crystal of 20-at. % Yb^{3+} doping concentration that we used in our experiments, these defects have a significant effect on the higher thermal loading in Yb:YAG and lower the laser efficiency. The laser cavity that we used was not optimized. At the same time, the shortest pulse duration can be obtained by use of the shortest laser cavity, so the higher peak power can be obtained.

4. Conclusions

The operation of a Ti:sapphire laser-pumped Yb:YAG passively Q-switched laser has been demonstrated at room temperature. We achieved a passively Q-switched pulse with energy of 3.2 μJ and a pulse duration of 350 ns. The highest average output power of 55 mW was obtained with a slope efficiency of approximately 15% and an optical efficiency of approximately 7%. Although the slope efficiency is low, by improving the Yb:YAG crystal quality to reduce defects, redesigning the oscillator cavity to shorten the cavity length, and adopting the more powerful diode laser to pump Yb:YAG crystal, we expect to increase the output power, peak power, and the conversion efficiency. Because of its high thermal, chemical, and optical stability, the Yb:YAG crystal can be considered to be useful as a passively Q-switched laser crystal for compact, efficient, and solid-state lasers.

This research was supported by the National Natural Science foundation of China under grant 6998806 and the National 863-416 Foundation of China. The valuable comments of the unidentified reviewers also had a beneficial effect on the final manuscript.

References

1. W. Koechner, *Solid-State Laser Engineering*, 3rd ed. (Springer-Verlag, New York, 1992), Chap. 8.
2. J. A. Morris and C. R. Pollock, "Passive Q-switching of a diode-pumped Nd:YAG laser with a saturable absorber," Opt. Lett. **15,** 440–442 (1990).
3. Y. Shimony, Z. Burshtein, A. Ben Amar-Baranga, Y. Kalisky, and M. Strauss, "Repetitive Q-switching of a cw Nd:YAG laser using Cr^{4+}:YAG saturable absorbers," IEEE J. Quantum Electron. **32,** 305–310 (1996).
4. S. E. Stokowski, M. H. Randles, and R. C. Morris, "Growth and characterization of large Nd,Cr:GSGG crystals for high-average-power slab lasers," IEEE J. Quantum Electron. **24,** 934–948 (1988).
5. M. I. Demchuk, V. P. Mikhailov, N. I. Zhavoronkov, N. V. Kuleshov, P. V. Prokoshin, K. V. Yumashev, M. G. Livshits, and B. I. Minkov, "Chromium-doped forsterite as a solid state saturable absorber," Opt. Lett. **17,** 929–930 (1992).
6. D. S. Sumida and T. Y. Fan, "Effect of radiation trapping on fluorescence lifetime and emission cross section measurements in solid-state laser media," Opt. Lett. **19,** 1343–1346 (1994).
7. T. Y. Fan, "Heat generation in Nd:YAG and Yb:YAG," IEEE J. Quantum Electron. **29,** 1457–1459 (1993).
8. S. L. Yellin, A. H. Shepard, R. J. Dalby, J. A. Baumaum, H. B. Serreze, T. S. Guide, R. Solarz, K. J. Bystrom, C. M. Harding, and R. G. Walters, "Reliability of GaAs-based semiconductor diode lasers: 0.6–1.1 μm," IEEE J. Quantum Electron. **29,** 2058–2067 (1993).
9. H. W. Bruesselbach, D. S. Sumida, R. A. Reeder, and R. W. Byren, "Low-heat high-power scaling using InGaAs-diode-pumped Yb:YAG lasers," IEEE J. Quantum Electron. **33,** 105–116 (1997).
10. T. Y. Fan, S. Klunk, and G. Henein, "Diode-pumped Q-switched Yb:YAG laser," Opt. Lett. **18,** 423–425 (1993).
11. G. J. Spühler, R. Paschotta, M. P. Kullberg, M. Graf, M. Moser, U. Keller, L. R. Brovelli, C. Harder, E. Mix, and G. Huber, "Passively Q-switched Yb:YAG microchip laser using a semiconductor saturable absorber mirror," in *Advanced Solid-State Lasers*, M. M. Fejier, H. Injeyan, and U. Keller, eds. Vol. 26 of OSA Trends in Optics and Photonics (Optical Society of America, Washington, D.C., 1999), pp. 187–189.
12. J. J. Zayhowski and P. L. Kelley, "Optimization of Q-switched lasers," IEEE J. Quantum Electron. **27,** 2220–2225 (1991).
13. J. J. Zayhowski and C. Dill III, "Diode-pumped passively Q-switched picosecond microchip lasers," Opt. Lett. **19,** 1427–1429 (1994).
14. H. Yin, P. Deng, and F. Gan, "Defects in YAG:Yb crystals," J. Appl. Phys. **83,** 3825–3828 (1998).
15. B. F. Aull and H. P. Jenssen, "Vibronic interactions in Nd:YAG resulting in nonreciprocity of absorption and stimulated emission cross section," IEEE J. Quantum Electron. **QE-18,** 925–930 (1982)
16. B. Peng and T. Izumitani, "Blue, green and 0.8 μm Tm^{3+}, Ho^{3+} doped upconversion laser glasses, sensitized by Yb^{3+}," Opt. Mater. **4,** 701–711 (1995).
17. J. C. Souriau, R. Romero, C. Borel, and C. Wyon, "Room-temperature dioide-pumped continuous-wave $SrY_4(SiO_4)O$:Yb^{3+},Er^{3+} crystal at 1554 nm," Appl. Phys. Lett. **64,** 1189–1191 (1994).